# THEORETICAL AND PRACTICAL RESEARCH ON THE FLEXURAL STRENGTH OF MASONRY

U. SCHMIDT
Dipl.-Ing., Research assistant and head of the working group "masonry"

J. HANNAWALD
Dr.-Ing. Dipl.-Phys., Research assistant and head of the working group "composite materials and modelling"

W. BRAMESHUBER
Prof. Dr.-Ing., Professor and Director
Institute of Building Materials Research (ibac), RWTH Aachen University, Germany

## SUMMARY

In this paper the results of the experimental investigations on the flexural load bearing behaviour of calcium silicate unit masonry as well as the results of investigations to determine the material laws of the single materials are presented.

## INTRODUCTION, ACKNOWLEDGEMENT

For the design of masonry building components subjected to flexural loads – these mainly include basement walls under stress from soil pressure or outer leaf of cavity walls and confined masonry walls under wind load – the flexural strength of masonry is required. Basically a differentiation is made between stress applied parallel and perpendicular to the bed joints. The flexural strength of masonry can be determined by tests on small wall specimens, which form a representative section of a large masonry wall. Appropriate calculation approaches taking into account the substantial material parameters of the units and the mortar as well as the geometrical boundary conditions do not exist so far. It is the aim of a research project currently carried out at the Institute of Building Materials Research (ibac) of RWTH Aachen University, Germany, to determine the stress distribution in masonry walls under flexural load and to develop a model for the flexural design. Therefore experimental and theoretical investigations (Finite Element Method) are conducted on small masonry walls. The material properties needed for the finite element calculations as e.g. full tensile stress-strain curves of the unit material and the mortar joint are determined in tests on small test specimens, in part newly developed by the authors. This paper reports on the hitherto existing results of the investigations. Due to the actual state of the project and the extensive investigations, this paper is restricted to the experimental investigations on masonry of solid calcium silicate units.

The research project is kindly financially supported by the Deutsche Forschungsgemeinschaft DFG (German Research Foundation).

## APPLIED MATERIALS AND CONDUCTED INVESTIGATIONS

The investigations were carried out on calcium silicate units without handling device but with a tongue and groove system, see Figure 1.

Figure 1. used calcium silicate units (498 mm x 175 mm x 248 mm)

A thin layer mortar and a general purpose mortar as well as an epoxy resin adhesive were applied as masonry mortar. The application of the different mortars and the resin, respectively, enables an examination of the relevant failure criteria at a joint failure as well as at a unit failure by means of the selected masonry units of one strength class. An essential part of the research project consists of tests on small specimens to determine the required material laws of the calcium silicate material and the bond properties of mortar and masonry unit for the subsequent numerical simulations of the walls. The material laws are partly determined directly from the experimental investigations, partly there is an inverse determination of the material laws by a numerical simulation of the small-size specimen tests. In altogether nine test series with two or three masonry walls, each, the flexural load bearing behaviour at a horizontal load transfer is examined. Here the essential parameters (overlap, filled and unfilled head joints) are varied on the states of stress and the load bearing behaviour in the masonry.

## MATERIAL LAWS OF THE UNITS

A survey of the tests conducted on the unit material as well as the test results are presented in Table 1. The tests are explained below.

The standardised compressive strength $f_{c,u}$ of the calcium silicate units was determined on solid masonry units. For the determination of the load deformation behaviour of the calcium silicate material under compressive loading and for the derivation of material laws, tests were carried out on slender calcium silicate cylinders (∅ = 100 mm, l = 200 mm) so that influences due to platen restraint were minimised. On the test specimens the axial and lateral deformations were determined with displacement transducers (DT) and a circumferential extensometer, respectively. Figure 2 shows a built-in test specimen, a typical fracture pattern as well as the determined stress-strain curves.

For the description of the load deformation behaviour under tensile load, cylinders (∅ = 100 mm, l = 200 mm) were drilled from the calcium silicate units in the direction of unit height and unit length. The load introduction was made by steel plates flexibly jointed and attached to the testing machine as well as glued onto to the test specimens. The load-dependent deformations were determined with DT. The test setup and the specific stress-

strain curves are illustrated in Figure 3. Additionally, the tensile strength was determined on the solid masonry units shown in Figure 1 in the direction of the unit length.

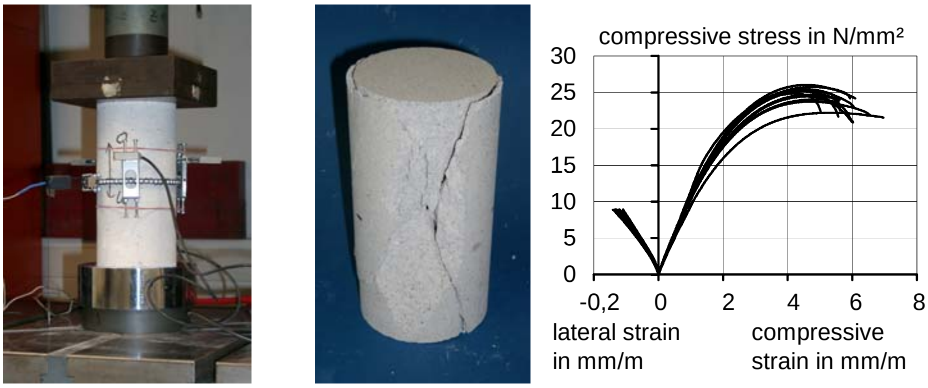


Figure 2. compression tests:
test setup, typical fracture pattern, compressive stress-strain curves

Table 1. Properties of the calcium silicate material (mean values)

| Test | Parameter | | Direction of unit | |
|---|---|---|---|---|
| | | | length | height |
| **Compression tests** | | | | |
| cylinder | compressive strength | $f_{c,cyl}$ [N/mm²] | | 24.7 |
| | modulus of elasticity | $E_{0c,cyl}$ [N/mm²] | - | 11750 |
| | Poisson´s ratio | $\nu_{33,cyl}$ [-] | | 0.15 |
| unit | compressive strength | $f_{c,u}$ [N/mm²] | | 25.1 |
| **Tension tests** | | | | |
| cylinder) | tensile strength | $f_{t,cyl}$ [N/mm²] | 2.69 | 3.30 |
| | modulus of elasticity | $E_{0t,cyl}$ [N/mm²] | 13320 | 13100 |
| unit | tensile strength | $f_{t,u}$ [N/mm²] | 1.96 N | - |
| **Flexural tests on prisms** | | | | |
| notch 10 mm | net flexural strength | $f_{fl,net}$ [N/mm²] | 3.50 | 3.22 |
| | fracture energy | $G_F$ [N/m] | 55.6 | 40.9 |
| unnotched | flexural strength | $f_{fl}$ [N/mm²] | 4.52 | 4.00 |
| **Flexural tests on units** | | | | |
| unnotched | flexural strength | $f_{fl,u}$ [N/mm²] | 4.30 | - |

To be able to determine the post-failure behaviour of the calcium silicate material under tensile load, deformation-controlled three-point bending tests (span 200 mm) were carried out on unnotched and notched prisms (notch depth 10 mm) with the dimensions of 200 · 40 · 40 mm³ taken in the direction of the masonry unit length and the unit height. The bending tests were simulated applying the Finite Element Method. By variation of the stress-crack opening relation in the numerical simulation, the load-deflection curves were adjusted in the best possible way to the experimental test results, cf. Schmidt et al. 2005 and Hannawald 2006, respectively, and thus the material law of the calcium silicate material was determined inversely. Figure 4 illustrates the test setup of the three-point bending test, the experimentally and numerically determined load-deflection curves as well as the inversely determined tensile stress-crack opening curves.

Furthermore, the flexural tensile strength was investigated on test specimens consisting of solid masonry units – several masonry units were glued together to obtain a sufficient

slenderness of the test specimens. At these tests a compensation for the specimens dead weight was made, cf. Schmidt et al. 2005.

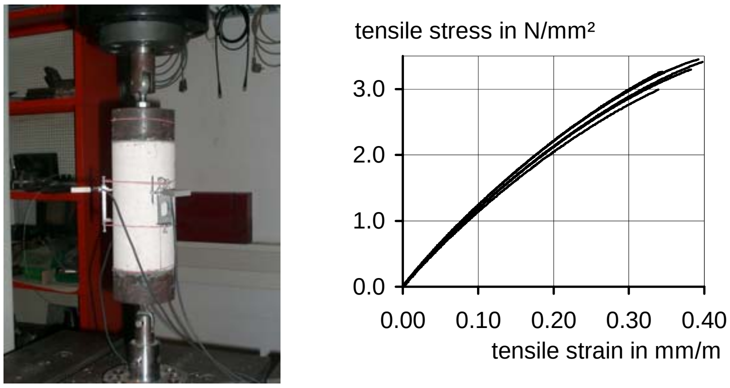


Figure 3. tension tests: test setup and tensile stress-strain curves

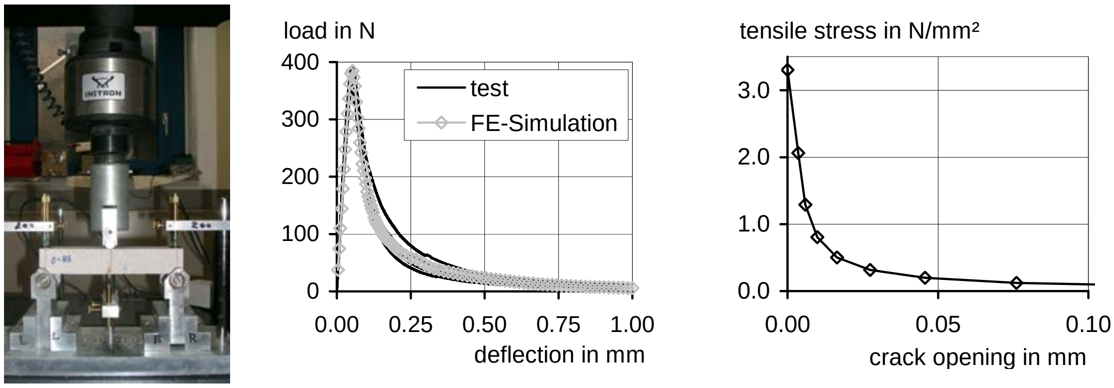


Figure 4. three-point bending tests:
test setup, load–deflection curve of 10 mm notched prisms, inversely determined tensile stress-crack opening relationship

## MATERIAL LAWS OF THE BOND

To describe the bond properties under tensile load, centric tensile bond tests were conducted on mortared cylinders taken from the masonry units. Figure 5 displays a test specimen as well as tensile stress-strain curves of thin layer mortar and general purpose mortar.

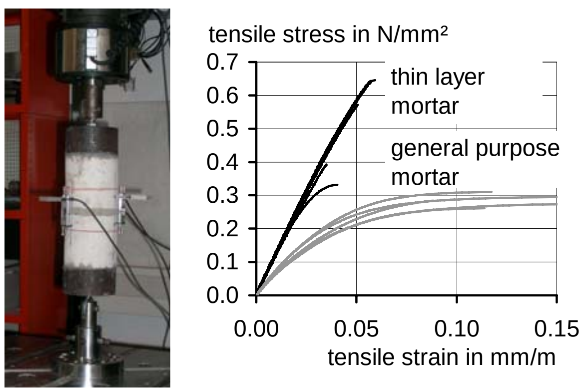


Figure 5. tensile bond tests: test setup and tensile stress-strain curve

The determination of the post-failure behaviour is made inversely by numerical simulation of three-point bending tests, analogous to the calcium silicate material. By mortaring together two sawn prism halves, test specimens with a mortar joint in the middle were manufactured analogous to Figure 4. By way of comparison, flexural tensile bond tests were conducted on mortared solid masonry units. The bond in the head joints as well as in the bed joints was examined. The test results are presented in Table 2.

Table 2. Properties of the bond (mean values)

| Test | Parameter | | Mortar | |
|---|---|---|---|---|
| | | | TLM | GPM |
| **Tension tests** | tensile bond strength | $f_t$ [N/mm²] | 0.53 | 0.28 |
| **Flexural tests** | | | | |
| prism (notch 10 mm) | net flex. tensile strength | $f_{fl,n}$ [N/mm²] | 0.67 | - |
| | flexural tensile strength | $f_{fl}$ [N/mm²] | 0.91 | 0.50 |
| prism (unnotched) | flexural tensile strength | $f_{fl}$ [N/mm²] | 1.09 | 0.42 |
| unit (bed joint, unnotched) | flexural tensile strength | $f_{fl}$ [N/mm²] | 1.02 | 0.29 |
| unit (head joint, unnotched) | | | | |

TLM – thin layer mortar, GPM – general purpose mortar

To describe the bond properties under shear stress, different test methods were applied. First the shear bond strength was determined according to the German respectively European Standards DIN 18 555-5 and EN 1052-3. Due to the irregular shear and axial stress distributions occurring in the joints, both test methods are not suitable for the direct determination of the actual material laws (shear stress-displacement curves). Basically an inverse determination with numerical simulation of the tests is possible, analogous to the flexural tensile tests. This procedure was chosen for instance in Schmidt et al. 2005. A test method which describes the stress in a bed joint of a wall under bending load more precisely is the determination of the torsional shear strength. The test setup presented in Schmidt and Schubert 2003 was refined in recent years (Klump 2004), so that also a test under simultaneous loading perpendicular to the bed joint is possible. Torsion tests with load perpendicular to the bed joint were carried out also by Willis in the recent past (Willis 2004). Within the framework of this project, extensive torsion tests were conducted on rectangular cross sections with different load levels. Even if the torsion of the masonry units in a wall under bending load can be better emulated by the torsional load of a rectangular section, these test specimens are not suitable to determine the actual material laws due to the complicated stress distribution. The determination of the actual material laws should also be made inversely here. A description of the results concerning the uniaxial shear bond strength and torsion shear strength on whole cross sections is therefore renounced in this place. Here the FE- calculations which still have to be conducted must be waited for.

According to the present state of knowledge, a direct determination of the material laws is possible with torsion tests on hollow cylinders because in these tests a defined state of stress develops in the test specimens. The torsion test setup as well as a test specimen drilled from a calcium silicate unit with thin layer mortar is illustrated in Figure 6. The first tests on solid and hollow cylinders, respectively, were conducted and published within the framework of the papers of Klump 2004 und Brameshuber et al. 2006. Comparable investigations which were carried out almost simultaneously, however completely independent of the own investigations, are described in Masia et al. 2006.

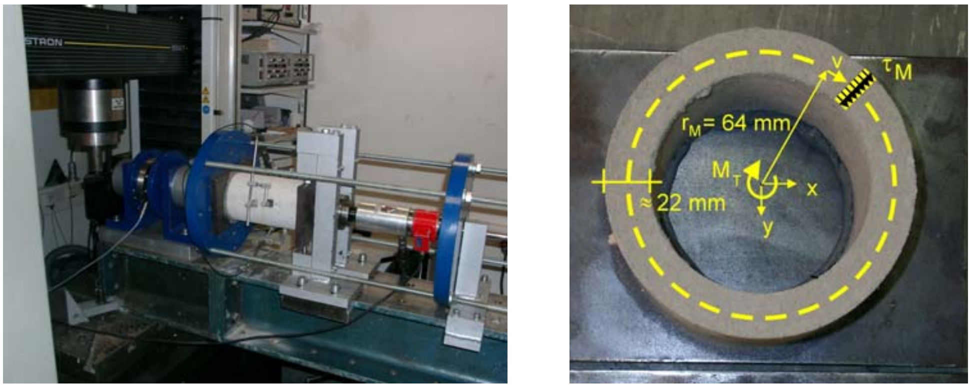


Figure 6. torsional tests: test set-up, test specimen

In Figure 7 the shear strength (mean values) depending on the precompression as well as the shear stress-deformation relations (related to the centre of the cross section $r_M$) for tests on calcium silicate units with thin layer mortar are exemplarily illustrated for different load levels. It can be assumed that the displayed shear stress-displacement curves describe the actual material laws so that the essential parameters – cohesion, initial and residual friction, fracture energy etc. - can be taken from them. For verification purposes also on this subject FE-simulations are conducted presently.

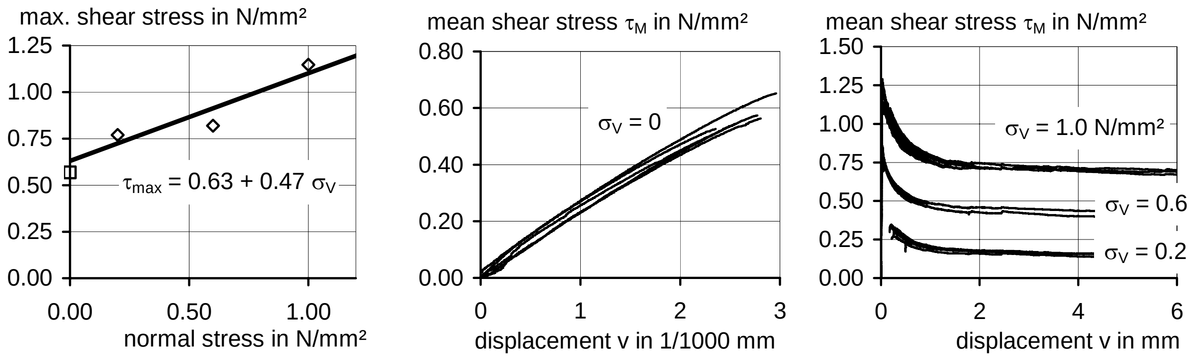


Figure 7. torsion tests:
max. shear stress vs. normal stress, mean shear stress - displacement curves of specimens without and with different precompression levels, respectively

## TESTS ON THE FLEXURAL BEHAVIOUR OF MASONRY

With the calcium silicate units displayed in Figure 1, small masonry walls (4 unit layers high and 4.5 unit lengths long) were built using thin layer mortar, general purpose mortar or epoxy resin. For each, the top layer and the bottom layer, masonry units which are halved in the direction of the unit height were used. The overlap amounted to either $l_0$ = 250 mm (half the unit length) or $l_0$ = 50 mm. Test series were made with filled and unfilled head joints with two or three test specimens, each. Figure 8 exemplarily illustrates a masonry wall with an overlap $l_0$ = 250 mm. Table 3 shows a survey of the conducted tests.

The investigation was made with a testing device as described in Schmidt and Schubert 2003. Deviating from this, the tests were conducted in a deformation-controlled way to be able to determine the post-failure behaviour, if necessary.

Table 3. Four-point bending tests on small masonry walls

| $l_0$ [mm] | Head joint | No. | Maximum load $F_{max}$ [kN] (failure mode: u – unit / j - joint) | | | Flexural tensile strength [N/mm²] | | |
|---|---|---|---|---|---|---|---|---|
| | | | epoxy | TLM | GPM | epoxy | TLM | GPM |
| 250 | un-filled | 1 | 34.6 (u) | 26.1 (j,u) | 15.3 (j) | 1.72 | 1.30 | 0.72 |
| | | 2 | 31.9 (u) | 27.1 (j,u) | 18.5 (j) | 1.56 | 1.32 | 0.89 |
| | | 3 | - | - | 20.2 (j) | - | - | 0.96 |
| | | mean | 17.8 | 26.6 | 18.0 | 1.64 | 1.31 | 0.86 |
| | filled | 1 | 46.6 (u) | - | 16.2 (j) | 2.31 | - | 0.,76 |
| | | 2 | 39.6 (u) | | 19.4 (j) | 1.95 | | 0.93 |
| | | 3 | 44.6 (u) | | 22.5 (j) | 2.22 | | 1.,07 |
| | | mean | 43.6 | | 19.4 | 2.16 | | 0.,92 |
| 50 | un-filled | 1 | 14.1 (u) | 7.4 (j) | - | 0.69 | 0.36 | - |
| | | 2 | 12.0 (u) | 7.6 (j) | | 0.59 | 0.37 | |
| | | mean | 13.1 | 7.5 | | 0.64 | 0.,37 | |
| | filled | 1 | 45.6 (u) | 12.3 (j) | - | 2.23 | 0.60 | - |
| | | 2 | 49.4 (u) | 13.7 (j) | | 2.41 | 0.67 | |
| | | mean | 47.5 | 13.0 | | 2.32 | 0.64 | |

TLM – thin layer mortar, GPM – general purpose mortar

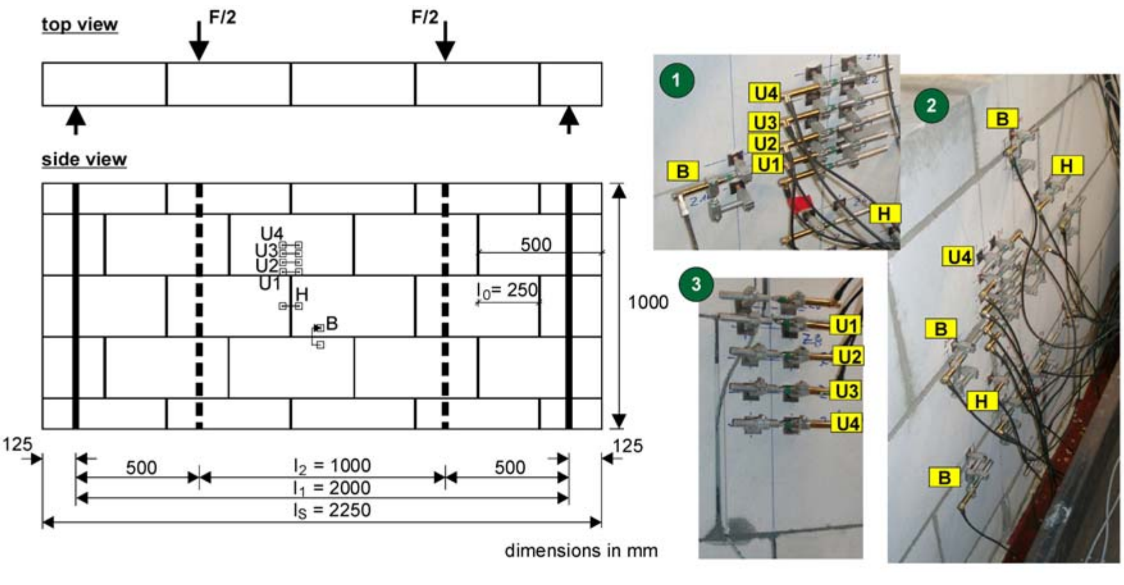


Figure 8. Four-point bending tests on small masonry walls

During testing the deflection in the centre of the wall (see Fig. 9) was measured considering the displacements of the supports. Furthermore comprehensive deformation measurements were carried out in the joint and masonry unit area to obtain knowledge regarding the states of stress and strain, respectively and to compare them later with the FE-calculations. For reasons of comparison, Figures 10 and 11 display deformation measurements which are explained in the following. The configuration of these selected measuring points is charted for the exemplarily shown wall geometry in Figure 8 on the left. The configuration of the measuring points was adjusted to the kind of failure to be expected as well as to the overlap. The pictures 1 to 3 in Figure 8 give an impression regarding the variation and number of the measuring points arranged at the single walls.

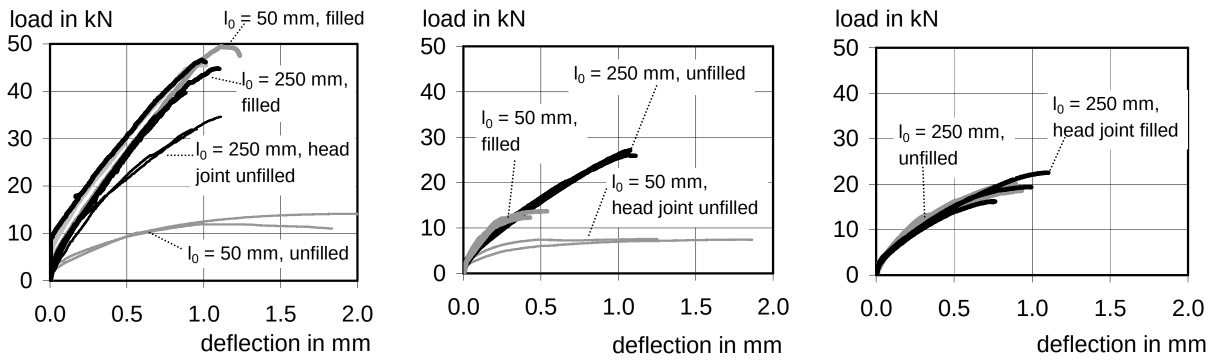


**Epoxy** **Thin layer mortar** **General purpose mortar**

Figure 9. Four-point bending tests on small masonry walls, load-deflection curves

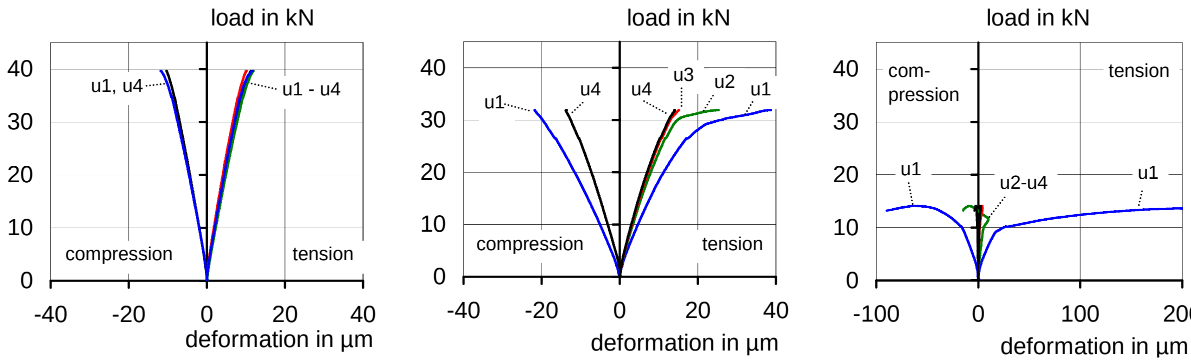


**head joint filled, $l_0$ = 250 mm** **head joint unfilled, $l_0$ = 250 mm** **head joint unfilled, $l_0$ = 50 mm**

Figure 10. Four-point bending tests on small masonry walls with epoxy deformation measurements on masonry units, number of LVDT see Fig. 8

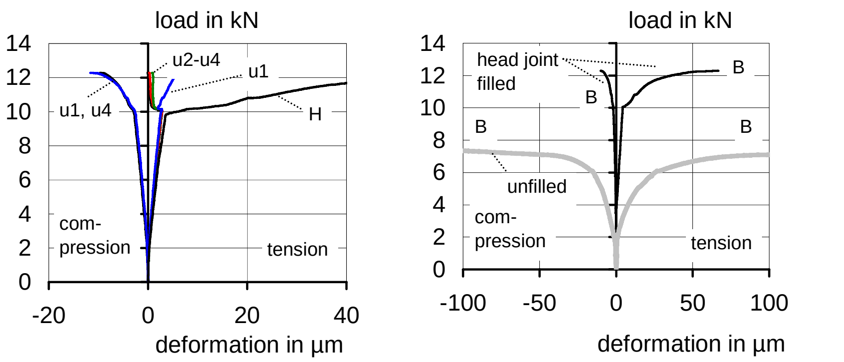


**head joint filled, $l_0$ = 50 mm** **head joint filled / unfilled $l_0$ = 50 mm**

Figure 11. Four-point bending tests on small masonry walls with thin layer mortar deformation measurements on masonry units, number of LVDT see Fig. 8

In Table 3 the maximum loads as well as the resulting values of the flexural tensile strength are stated. During the tests, by means of the deformation measurements in the masonry unit and joint area, an influence of the friction at the wall base on the load bearing behaviour could be identified which was partly different in the single tests. The maximum deviation related to the maximum load as a result of the above mentioned friction amounts to between about 0 to 8 %. This effect remains unconsidered at first in the further evaluation. In the following some preliminary evaluations of the test results are demonstrated.

At the test specimens which are glued with epoxy resin and which have filled head joints, no significant influence of the overlap on the load-deflection curves can be discerned. The masonry walls can be regarded as homogeneous. The flexural tensile strength is distinctly lower compared to the masonry units ($f_{fl,u}$ = 4.30 N/mm²). This has presumably mainly to be ascribed to the verifiably lower strengths of the masonry units in the near-surface region of the head joint. At the walls, the masonry units failed in this region. In Figure 10 on the left, the deformation measurements in the masonry unit area show no difference between the measuring points at the edge region (U1) and in the centre (U4) of the masonry unit until failure occurs. This is also an indication for the homogeneity of the masonry. At unfilled head joints (see Fig. 10, middle, for $l_0$ = 250 mm), stress concentrations occur in the edge region of the masonry unit above and below the open head joints which lead to significantly higher measured deformations of the measuring points near the edges (U1). The non-linear gradient at these measuring points indicates a beginning crack formation at the edge region of the masonry units. Reducing the overlap, this effect is increased substantially (see Fig. 10, right, for $l_0$ = 50 mm) – here, the corner of the unit has broken off (see picture 3 in Fig. 8) -, which also leads to considerably lower wall strengths. It is discernible that the crack formation in the edge region of the masonry units leads to clearly non-linear load-deflection curves (see head joint, unfilled, Fig. 9, left), however, it does not lead directly to a wall failure. In this connection, the importance of the knowledge regarding the post-failure behaviour of the building materials becomes obvious.

In Figure 11 on the left it can be observed that, the wall with thin layer mortar and filled head joints ($l_0$ = 50 mm), up to $F \approx 10$ kN the measured deformations in the area of the masonry units and the head joints are approximately equal and that the masonry can be regarded as “homogeneous”, analogous to Figure 10, left. At $F \approx 10$ kN the bond between the head joints fails – this becomes apparent in the deformation increase at the measuring point H. On the tension side, the gaping of the head joints leads to stress concentrations in the edge region of the masonry units which can be seen from the deformation increase at the measuring point U1. As a result of the short overlap, the deformations at the measuring points U2, U3 and U4 amount to almost 0 on the tension side, analogous to Figure 10, right. Because of the mortaring of the head joints, a compressive stress transmission in the head joints is furthermore possible. This leads to the same deformations at the measuring points U1 and U4 on the compression side. Even here, the non-linear gradient from the time of the opening of the head joints can clearly be seen. The failure of the bond in the head joints leads to torsion of the masonry units in the wall – i. e. a torsional load of the bed joints – which can be discerned from a significant increase in the mutual displacement of masonry units lying on top of each other (see Fig. 11, right). At unfilled head joints, the mutual torsion is already considerably higher immediately after starting loading. Moreover, due to the compressive stress transmission in the head joints, the centre of rotation is also not in the middle axis of the wall, contrary to unfilled head joints. This becomes apparent in the different deformations on the compression and the tension side upon failure of the head joint. The failure of the head joints is also reflected in the load-deflection curves (see Fig. 9, middle) in the change of the gradient at about $F \approx 10$ kN. Already at Willis 2004 and van der Pluim 1999 such changes in the gradients of load-deflection curves were ascribed to a failure of the head joints. These mechanisms are now comprehensible as a result of the deformation measurements in the masonry unit and joint area. The fact that the flexural tensile stress at the gaping of the head joints is here only about half as large as the flexural tensile bond strength in the test on the small-size test specimens ($f_{fl}$ = 1,02 N/mm²) can at first be ascribed to phenomena due to the manufacturing.

For the general purpose mortar, no difference between the load-deflection curves of filled and of unfilled head joints can be discerned (see Fig. 9, left). It can be assumed that already at very small loads no tensile stresses in the head joint can be transmitted. As a result of the compressive stress transmission, higher flexural tensile strengths could however have been expected. At comparative shear bond tests that were conducted for each mortar mix it became however obvious that the bond strength of the mixes used in the masonry walls with the filled head joints was lower. This must be considered when evaluating the experimental results.

## SUMMARY AND OUTLOOK

In the small-size specimen tests the material laws of the calcium silicate masonry units and bond, especially the post-failure behaviour, were determined. The experimental tests on the masonry walls with extensive deformation measurements enable a reconstruction of the failure mechanisms under bending load and demonstrate the importance of the knowledge regarding the post-failure behaviour of the single building materials. The determined material laws are the basis for the parameters for the FE-simulations which are currently being conducted and calibrated according to the present results of the masonry wall tests.

## REFERENCES

Brameshuber, W. ; Graubohm, M. ; Schmidt, U.: Festigkeitseigenschaften von Mauerwerk. Teil 4: Scherfestigkeit. Berlin : Ernst & Sohn. - In: Mauerwerk-Kalender 31 (2006), S. 193-225 – (in German)

DIN 18 555-5 03.86. Prüfung von Mörteln mit mineralischen Bindemitteln; Festmörtel. Bestimmung der Haftscherfestigkeit von Mauermörteln

EN 1052-3:2002/prA1:2004 (E) Methods of test for masonry - Part 3: Determination of initial shear strength

Hannawald, J.: Determining the Tensile Softening Diagram of Concrete-Like Materials Using Hybrid Optimisation. Dordrecht : Springer, 2006. - In: Measuring, Monitoring and Modeling Concrete Properties. An International Symposium Dedicated to Prof. Surendra P. Shah, Northwestern University, USA, (Konsta-Gdoutos, M.S. (Ed.)), S. 179-187

Klump, J.: Untersuchungen zur Torsionsscherfestigkeit von Mauerwerkprüfkörpern : Determination of the Torsional Shear Strength on Masonry Test Specimen. Aachen, Technische Hochschule, Fachbereich 3, Institut für Bauforschung, master thesis, 2004. - (not published, in German)

Masia, M.J. ; Han, Y. ; Correa, M.R.S.: Torsion Testing for the Characterisation of the Shear Behaviour of Mortar Joints in Masonry. In: Masonry International Journal of the British Masonry Society 19 (2006), Nr. 2, S. 77-88

Pluijm van der, R.: Out-of-Plane Bending of Masonry Behaviour and Strength. Eindhoven, Technische Universiteit, Proefschrift, 1999

Schmidt, U. ; Schubert, P.: Flexural Strength of Masonry. Madison : Omnipress, 2003. - In: Proceedings of the Ninth North American Masonry Conference, Clemson University of Clemson, South Carolina, June 1-4, 2003, S. 674-685

Schmidt, U. ; Beer, I. ; Brameshuber, W.: Tests on the Load Bearing Behaviour of Masonry Shear Walls. Calgary : Department of Civil Engineering, 2005. - In: Proceedings of the 10th Canadian Masonry Symposium, Banff, Alberta, Canada, June 8-12, 2005, S. 704-713

Willis, C.R.: Design of Unreinforced Masonry Walls for Out-of-Plane Loading. Adelaide, University of Adelaide, School of Civil and Environment Engineering, Thesis, 2004